



Available online at www.sciencedirect.com

SCIENCE @ DIRECT®

C. R. Mecanique 331 (2003) 401–406



Electrophoresis of a 2-particle cluster near a plane boundary

Antoine Sellier

LadHyX, École polytechnique, 91128 Palaiseau cedex, France

Received 27 May 2002; accepted after revision 2 May 2003

Presented by Paul Germain

Abstract

Particle-boundary and particle-particle interactions in Electrophoresis are examined by considering a 2-particle cluster near a plane boundary. The advocated treatment holds for two insulating particles of arbitrary shapes and zeta potential functions and resorts to 13 boundary-integral equations. Preliminary results reveal that, depending upon the addressed velocity nature (translational or angular), wall-particle may be stronger or weaker than particle-particle interactions. *To cite this article: A. Sellier, C. R. Mecanique 331 (2003).*

© 2003 Académie des sciences. Published by Éditions scientifiques et médicales Elsevier SAS. All rights reserved.

Résumé

Electrophorèse de deux particules en présence d'une paroi plane. On examine l'électrophorèse d'une particule isolante, sous l'action d'un champ électrique uniforme \mathbf{E}_∞ , en présence d'une seconde particule isolante et d'une paroi plane parfaitement conductrice et normale à \mathbf{E}_∞ ou isolante et parallèle à \mathbf{E}_∞ . La méthode préconisée utilise 13 équations intégrales de frontière et on montre que, selon la nature (translation ou rotation) de la vitesse examinée, les interactions paroi-particule peuvent être plus fortes ou moindres que les interactions particule-particule. *Pour citer cet article : A. Sellier, C. R. Mecanique 331 (2003).*

© 2003 Académie des sciences. Published by Éditions scientifiques et médicales Elsevier SAS. All rights reserved.

Keywords: Fluid mechanics; Electrophoresis; Wall-particle interactions; Particle-particle interactions

Mots-clés : Mécanique des fluides ; Electrophorèse ; Paroi plane ; Interactions

Version française abrégée

On place au dessus du plan Σ , d'équation $x_3 = 0$ en coordonnées cartésiennes $x_j = \mathbf{OM} \cdot \mathbf{e}_j$, deux particules solides \mathcal{P}_n ($n = 1, 2$) dans un électrolyte de viscosité μ et permittivité ϵ uniformes (voir la Fig. 1). La surface isolante \mathcal{S}_n de \mathcal{P}_n admet le zéta potentiel ζ_n et sous le champ électrique \mathbf{E}_∞ uniforme \mathcal{P}_n acquiert une vitesse de translation $\mathbf{U}^{(n)}$ (celle d'un point O_n de \mathcal{P}_n) et de rotation $\boldsymbol{\Omega}^{(n)}$, fonctions de $\epsilon\mathbf{E}/\mu$, O_1O_2 , $h_n = \mathbf{OO}_n \cdot \mathbf{e}_3$, ζ_n et du plan Σ : isolant, de zéta potentiel uniforme ζ_w et parallèle à \mathbf{E}_∞ (Cas 1) ou parfaitement conducteur et normal à \mathbf{E}_∞ (Cas 2). Les cas d'une sphère sans [2–5] ou avec [9–12] Σ et de deux sphères [6–8] sans Σ ont été

E-mail address: sellier@ladhyx.polytechnique.fr (A. Sellier).

résolus (avec ζ_1 et ζ_2 uniformes sauf dans [12]). Cette Note envisage deux particules de formes et de zéta potentiels arbitraires en présence de Σ .

Dans le domaine fluide Ω le champ électrique est $\mathbf{E} = \mathbf{E}_\infty - \nabla\phi$. Le potentiel ϕ et l'écoulement (\mathbf{u}, p) , de tenseur des contraintes σ , vérifient [10] le problème (2)–(5) où \mathbf{n} est la normale sortante sur $\mathcal{S} = \mathcal{S}_1 \cup \mathcal{S}_2$ et $r = OM$. La particule \mathcal{P}_n d'inertie négligeable migre librement ce qui conduit [1] à (6). Le théorème de réciprocité [13] étendu aux 12 écoulements de Stokes $(\mathbf{u}_L^{(n),i}, p_L^{(n),i})$, assujettis pour $L \in \{T, R\}$ à (7) où δ est le symbol de Kronecker et induisant sur \mathcal{S} les efforts surfaciques $\mathbf{f}_L^{(n),i}$, permet de réécrire (2)–(6) sous la forme de (8), (9) avec $\zeta' = \zeta_n - \zeta_w$ sur \mathcal{S}_n (Cas 1) ou $\zeta' = \zeta_n$ sur \mathcal{S}_n (Cas 2) et $U_j^{(n)} = \mathbf{U}^{(n)} \cdot \mathbf{e}_j$, $\Omega_j^{(n)} = \boldsymbol{\Omega}^{(n)} \cdot \mathbf{e}_j$. Le système (8), de matrice symétrique et définie négative [13], admet une solution unique $(\mathbf{U}^{(1)}, \boldsymbol{\Omega}^{(1)}, \mathbf{U}^{(2)}, \boldsymbol{\Omega}^{(2)})$ obtenue en calculant $\nabla\phi$ et $\mathbf{f}_L^{(n),i}$ sur \mathcal{S} par résolution numérique de 13 équations intégrales de Fredholm de seconde ((10)) ou de première ((11); voir [15]) espèce si $M'(x_1, x_2, -x_3)$ est le symétrique de $M(x_1, x_2, x_3)$ par rapport à Σ . En effet, l'approximation de ϕ via (10) et donc de ses dérivées tangentielles conduit, grâce à $\nabla\phi \cdot \mathbf{n} = \mathbf{E}_\infty \cdot \mathbf{n}$, à celle de $\nabla\phi$ sur \mathcal{S} . La discréétisation (isoparamétrique avec un maillage à N_n noeuds de triangles curvilignes sur \mathcal{S} [16]) de (10), (11) débouche sur des systèmes linéaires traités par factorisation LU .

Pour $\mathbf{E}_\infty = E\mathbf{e}_1 \neq \mathbf{0}$ (Cas 1) et deux sphères de rayon a , de centres O_n et de zéta potentiels uniformes ζ_n astreints à (14), traçons les mobilités non nulles $u_i^{(n)}(d, \lambda)$ et $w_i^{(n)}(d, \lambda)$, introduites par (15), où d et λ sont des paramètres de séparation sphère–sphère et Σ -sphère. Notons que pour \mathcal{P}_n seule (voir (1)) $u_i^{(n)}(0, 0) = \delta_{i1}\delta_{n1}$, $w_i^{(n)}(0, 0) = 0$ à savoir que $u_i^{(n)}(d, \lambda) - \delta_{i1}\delta_{n1}$ et $w_i^{(n)}(d, \lambda)$ représentent l'influence des seules interactions paroi–sphère (ΣS) si $d = 0$ et combinées paroi–sphère et sphère–sphère ($\Sigma S - SS$) si $d > 0$ sur la migration de \mathcal{P}_n seule. Les cas d'une sphère avec Σ ($d = 0$, [11]) et de deux sphères sans Σ ($\lambda = 0$, [7]) montrent (voir le Tableau 1) que le choix $N_1 = N_2 = 866$ assure une précision de l'ordre de 5×10^{-4} pour $\text{Max}(d, \lambda) \leqslant 0,9$. La Fig. 2 procure sous ce choix, en fonction de λ et pour $d = 0; 0,3; 0,6; 0,8$ et $0,9$, les seules fonctions non nulles $u_1^{(n)}$, $w_2^{(2)}$, $w_2^{(1)}(0, \lambda)$ et $w_2'^{(1)}(d, \lambda) = 10[w_2^{(1)}(0, \lambda) - w_2^{(1)}(d, \lambda)]$ si $d > 0$. Les interactions combinées $\Sigma S - SS$ sont ainsi plus importantes pour $u_1^{(n)}$ et $w_2^{(2)}$ (voir Figs. 2(a), (b), (d)) mais moindres pour $w_2^{(1)}$ (voir Fig. 2(c)) que les interactions ΣS . Les interactions paroi–sphère sont faibles pour $u_1^{(n)}$ (à d fixé $u_1^{(n)}$ varie peu avec λ aux Figs. 2(a) et (b)) et les interactions combinées $\Sigma S - SS$, positives pour $u_1^{(1)}$ et négatives pour $u_1^{(2)}$, croissent jusqu'à 20% avec d . A l'opposé, pour $w_2^{(n)}$ les interactions $\Sigma S - SS$ s'avèrent faibles (au plus 3%), positives pour \mathcal{P}_1 (voir $w_2'^{(1)}$) mais positives ou négatives pour \mathcal{P}_2 (voir $w_2^{(2)}$).

1. Introduction

We consider two solid and insulating particles \mathcal{P}_n ($n = 1, 2$) freely suspended above a plane boundary Σ in a viscous electrolyte of constant dielectric permittivity ϵ and viscosity μ (see Fig. 1).

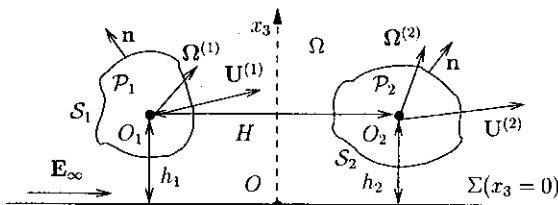


Fig. 1. Two solid particles \mathcal{P}_1 and \mathcal{P}_2 lying near the insulating plane Σ .

Fig. 1. Deux particules solides \mathcal{P}_1 et \mathcal{P}_2 au voisinage du plan isolant Σ .

Particle-electrolyte interactions induce on the surface S_n of \mathcal{P}_n a so-called “zeta potential” function ζ_n and applying a uniform external electric field \mathbf{E}_∞ results in a motion of \mathcal{P}_n [1] of unknown translational velocity $\mathbf{U}^{(n)}$ (the velocity of one point O_n of \mathcal{P}_n) and angular velocity $\boldsymbol{\Omega}^{(n)}$. Since this migration, termed electrophoresis, plays a key role in particle analysis and/or separation it is of prime interest to determine $(\mathbf{U}^{(n)}, \boldsymbol{\Omega}^{(n)})$. If $h_n = d(O_n, \Sigma)$ and $H = O_1 O_2$ respectively denote typical \mathcal{P}_n -wall and $\mathcal{P}_1 - \mathcal{P}_2$ separations, available works [2–12] only deal, for \mathbf{E}_∞ uniform, with the following cases:

- (i) A single particle $\mathcal{P}_1 (h_1 = h_2 = H = \infty)$. If ζ_1 is uniform the Smoluchowski solution

$$\mathbf{U}^{(1)} = \varepsilon \zeta_1 \mathbf{E}_\infty / \mu, \quad \boldsymbol{\Omega}^{(1)} = 0 \quad (1)$$

holds [2–4]. If ζ_1 is non-uniform \mathcal{P}_1 may both rotate and translate [5].

- (ii) Two particles without boundaries ($h_1 = h_2 = \infty$). Such circumstances focus on $\mathcal{P}_1 - \mathcal{P}_2$ interactions and has only received attention for two spheres of uniform ζ_n [6–8].
- (iii) One particle \mathcal{P}_1 near a plane wall Σ ($H = \infty$). The available literature ([9–11] for a sphere with ζ_1 uniform and [12] for any shape and ζ_1 function) handles two cases:
Case 1: Σ is insulating, of uniform zeta potential ζ_w and parallel to \mathbf{E}_∞ .
Case 2: Σ is normal to \mathbf{E}_∞ and perfectly conducting.

This Note extends the method advocated in [12] to a 2-particle cluster near the wall Σ in above Cases 1 and 2. It also both encloses and discusses our preliminary results.

2. Relevant boundary-integral equations and numerical treatment

We use cartesian coordinates $x_j = \mathbf{OM} \cdot \mathbf{e}_j$ with Σ located at $x_3 = 0$ and the usual summation convention with $r = OM = (x_j x_j)^{1/2}$, $\mathbf{U}^{(n)} = U_j^{(n)} \mathbf{e}_j$ and $\boldsymbol{\Omega}^{(n)} = \Omega_j^{(n)} \mathbf{e}_j$. In the fluid domain Ω the electric field becomes $\mathbf{E} = \mathbf{E}_\infty - \nabla \phi$. If \mathbf{n} denotes the unit outward normal on $\mathcal{S} = \mathcal{S}_1 \cup \mathcal{S}_2$ the perturbation potential ϕ and the fluid flow (\mathbf{u}, p) obey [10]

$$\nabla^2 \phi = \nabla \cdot \mathbf{u} = 0 \quad \text{and} \quad \mu \nabla \mathbf{u} = \nabla p \quad \text{in } \Omega, \quad (\nabla \phi, p) \rightarrow (0, 0) \quad \text{as } r \rightarrow \infty \quad (2)$$

$$\nabla \phi \cdot \mathbf{n} = \mathbf{E}_\infty \cdot \mathbf{n} \quad \text{and} \quad \mathbf{u} = \mathbf{U}^{(n)} + \boldsymbol{\Omega}^{(n)} \wedge \mathbf{O}_n \mathbf{M} - \varepsilon \zeta_n \mathbf{E} / \mu \quad \text{on } S_n \quad (3)$$

$$\text{Case 1: } \nabla \phi \cdot \mathbf{e}_3 = \mathbf{E}_\infty \cdot \mathbf{e}_3 = 0 \quad \text{and} \quad \mathbf{u} = -\frac{\varepsilon \zeta_w}{\mu} \mathbf{E} \quad \text{on } \Sigma, \quad \mathbf{u} \rightarrow -\frac{\varepsilon \zeta_w}{\mu} \mathbf{E}_\infty \quad \text{as } r \rightarrow \infty \quad (4)$$

$$\text{Case 2: } \phi = 0 \quad \text{and} \quad \mathbf{u} = \mathbf{0} \quad \text{on } \Sigma, \quad \mathbf{u} \rightarrow \mathbf{0} \quad \text{as } r \rightarrow \infty \quad (5)$$

According to [1], \mathbf{E} applies zero net force and torque on the freely-suspended particle \mathcal{P}_n . If $\sigma = \sigma(\mathbf{u}, p)$ denotes the stress tensor one thus supplements (2)–(5) with the relations

$$\int_{S_n} \mathbf{e}_i \cdot \sigma \cdot \mathbf{n} dS_n = 0; \quad \int_{S_n} [\mathbf{e}_i \wedge \mathbf{O}_n \mathbf{M}] \cdot \sigma \cdot \mathbf{n} dS_n = 0 \quad \text{for } i \in \{1, 2, 3\}, n \in \{1, 2\} \quad (6)$$

For $L \in \{T, R\}$, let us consider twelve Stokes flows $(\mathbf{u}_L^{(n),i}, p_L^{(n),i})$ such that

$$\mathbf{u}_L^{(n),i} = \mathbf{0} \quad \text{on } \Sigma \quad \text{and} \quad \text{as } r \rightarrow \infty, \quad \mathbf{u}_T^{(n),i} = \delta_{nm} \mathbf{e}_i \quad \text{and} \quad \mathbf{u}_R^{(n),i} = \delta_{nm} [\mathbf{e}_i \wedge \mathbf{O}_n \mathbf{M}] \quad \text{on } S_m \quad (7)$$

where δ denotes the Kronecker delta and subscripts T or R respectively hold for a translation or a rotation of \mathcal{P}_n . Designating by $\mathbf{f}_L^{(n),i}$ the surface stress induced on \mathcal{S} by $(\mathbf{u}_L^{(n),i}, p_L^{(n),i})$ and extending to our multiply-connected

and semi-infinite domain Ω the Lorentz reciprocal theorem [13], one arrives, under velocity boundary conditions (3)–(5), at the equations

$$A_{(m),L}^{(n),i,j} U_j^{(m)} + B_{(m),L}^{(n),i,j} \Omega_j^{(m)} = \frac{\epsilon}{\mu} \int_S \zeta' [\mathbf{E}_\infty - \nabla \phi] \cdot \mathbf{f}_L^{(n),i} dS \quad (8)$$

with $\zeta' = \zeta_n - \zeta_w$ on S_n in Case 1, $\zeta' = \zeta_n$ on S_n in Case 2 and

$$A_{(m),L}^{(n),i,j} = \int_{S_m} \mathbf{e}_j \cdot \mathbf{f}_L^{(n),i} dS_m, \quad B_{(m),L}^{(n),i,j} = \int_{S_m} (\mathbf{e}_j \wedge \mathbf{O}_m \mathbf{M}) \cdot \mathbf{f}_L^{(n),i} dS_m \quad (9)$$

Note [13] that (8) admits a symmetric and negative-definite 12×12 matrix. By virtue of (8), (9), the unique solution $(\mathbf{U}^{(1)}, \boldsymbol{\Omega}^{(1)}, \mathbf{U}^{(2)}, \boldsymbol{\Omega}^{(2)})$ is gained by evaluating $\nabla \phi$ and $\mathbf{f}_L^{(n),i}$ on $S = S_1 \cup S_2$ only. If $M'(x_1, x_2, -x_3)$ is the symmetric of $M(x_1, x_2, x_3)$ with respect to the plane Σ , the function ϕ obeys in Case l ($l = 1, 2$) the boundary-integral equation

$$\begin{aligned} & -4\pi\phi(M) + \int_S [\phi(P) - \phi(M)] \frac{\mathbf{P}\mathbf{M} \cdot \mathbf{n}(P)}{PM^3} dS_P + (-1)^{l+1} \int_S \phi(P) \frac{\mathbf{P}\mathbf{M}' \cdot \mathbf{n}(P)}{PM'^3} dS_P \\ &= \int_S [\mathbf{E}_\infty \cdot \mathbf{n}](P) \left\{ \frac{1}{PM} + (-1)^{l+1} \frac{1}{PM'} \right\} dS_P \end{aligned} \quad (10)$$

A non-trivial generalization to two particles of results established for one particle [14,15] shows that the required surface stress $\mathbf{f}_L^{(n),i}$ fulfills the boundary-integral equation

$$-8\pi\mu[\mathbf{u}_L^{(n),i} \cdot \mathbf{e}_j](M) = \int_S [G_{jk}^0 + G_{jk}^b](P, M) [\mathbf{f}_L^{(n),i}(P) \cdot \mathbf{e}_k] dS_P \quad (11)$$

$$G_{jk}^0(P, M) = \delta_{jk}/PM + (\mathbf{P}\mathbf{M} \cdot \mathbf{e}_j)(\mathbf{P}\mathbf{M} \cdot \mathbf{e}_j)/PM^3 \quad (12)$$

$$\begin{aligned} G_{jk}^b(P, M) &= G_{jk}^0(P, M') - 2c_j[(\mathbf{O}\mathbf{M} \cdot \mathbf{e}_3)/PM'^3] \\ &\times \{\delta_{k3}\mathbf{P}\mathbf{M}' \cdot \mathbf{e}_j - \delta_{j3}\mathbf{P}\mathbf{M}' \cdot \mathbf{e}_k + \mathbf{O}\mathbf{P} \cdot \mathbf{e}_3[\delta_{jk} - 3(\mathbf{P}\mathbf{M}' \cdot \mathbf{e}_j)(\mathbf{P}\mathbf{M}' \cdot \mathbf{e}_k)/PM'^2]\} \end{aligned} \quad (13)$$

with $c_1 = c_2 = 1$, $c_3 = -1$. Thus, inverting one and twelve Fredholm boundary-integral equations (10) and (11) respectively yields ϕ and $\mathbf{f}_L^{(n),i}$ on S . The numerical implementation uses a N_n -node mesh of isoparametric, curvilinear and triangular 6-node boundary elements on S_n [16] and solves the linear systems associated to (10), (11) by Gaussian elimination. Finally, $\nabla \phi$ is deduced on S from the link $\nabla \phi \cdot \mathbf{n} = \mathbf{E}_\infty \cdot \mathbf{n}$ and the calculation of its tangential derivatives from the numerical approximation of ϕ .

3. Preliminary results and discussion

We report numerical results for an “horizontal” 2-sphere cluster with $\mathbf{E}_\infty = E\mathbf{e}_1 \neq \mathbf{0}$ (Case 1). Each sphere P_n has radius a , center O_n and uniform zeta potential ζ_n with

$$\mathbf{O}\mathbf{O}_n = \frac{(-1)^n a}{d} \mathbf{e}_1 + \frac{a}{\lambda} \mathbf{e}_3, \quad 0 \leq d < 1, \quad 0 \leq \lambda < 1, \quad \zeta'_1 = \zeta_1 - \zeta_w \neq 0, \quad \zeta'_2 = \zeta_2 - \zeta_w = 0 \quad (14)$$

where d and λ denote sphere–sphere and sphere–wall separation parameters. The case of ζ'_1 and ζ'_2 uniform and non-zero may be easily deduced from the above choice of (ζ'_1, ζ'_2) by symmetry properties. Non-zero and so-called electrophoretic “mobilities”

$$u_i^{(n)}(d, \lambda) = \mu[\mathbf{U}^{(n)} \cdot \mathbf{e}_i]/[\epsilon E \zeta'_1], \quad w_i^{(n)}(d, \lambda) = \mu[\boldsymbol{\Omega}^{(n)} \cdot \mathbf{e}_i]/[\epsilon E \zeta'_1] \quad (15)$$

are computed with $N = 2N_1 = 2N_2$ collocations points on $\mathcal{S} = \mathcal{S}_1 \cup \mathcal{S}_2$. If $\lambda = 0$ or $d = 0$ one recovers circumstances (ii) or (iii) (two spheres free from boundaries or one sphere with a plane boundary). As shown in Table 1, using a refined 866-node mesh on each sphere yields numerical errors of order of 5×10^{-4} in the range $\text{Max}(d, \lambda) \leq 0.9$.

Table 1

Comparison between theoretical [7,11] and computed non-zero mobilities $u_1^{(1)}(0, 0.9)$, $w_2^{(1)}(0, 0.9)$ and $u_1^{(1)}(0.9, 0)$ for different settings $N_1 = N_2$

Tableau 1

Mobilités non nulles $u_1^{(1)}(0; 0.9)$, $w_2^{(1)}(0; 0.9)$ et $u_1^{(1)}(0.9; 0)$ pour différents choix de $N_1 = N_2$. Comparaisons avec [7,11]

$N_1 = N_2$	$u_1^{(1)}(0, 0.9)$	$u_1^{(1)}[11]$	$w_2^{(1)}(0, 0.9)$	$w_2^{(1)}[11]$	$u_1^{(1)}(0.9, 0)$	$u_1^{(1)}[7]$
74	0.99869	0.99789	-0.20454	-0.20389	0.82046	0.79031
242	0.99625	0.99789	-0.20563	-0.20389	0.79455	0.79031
530	0.99794	0.99789	-0.20354	-0.20389	0.79199	0.79031
866	0.99779	0.99789	-0.20338	-0.20389	0.79023	0.79031

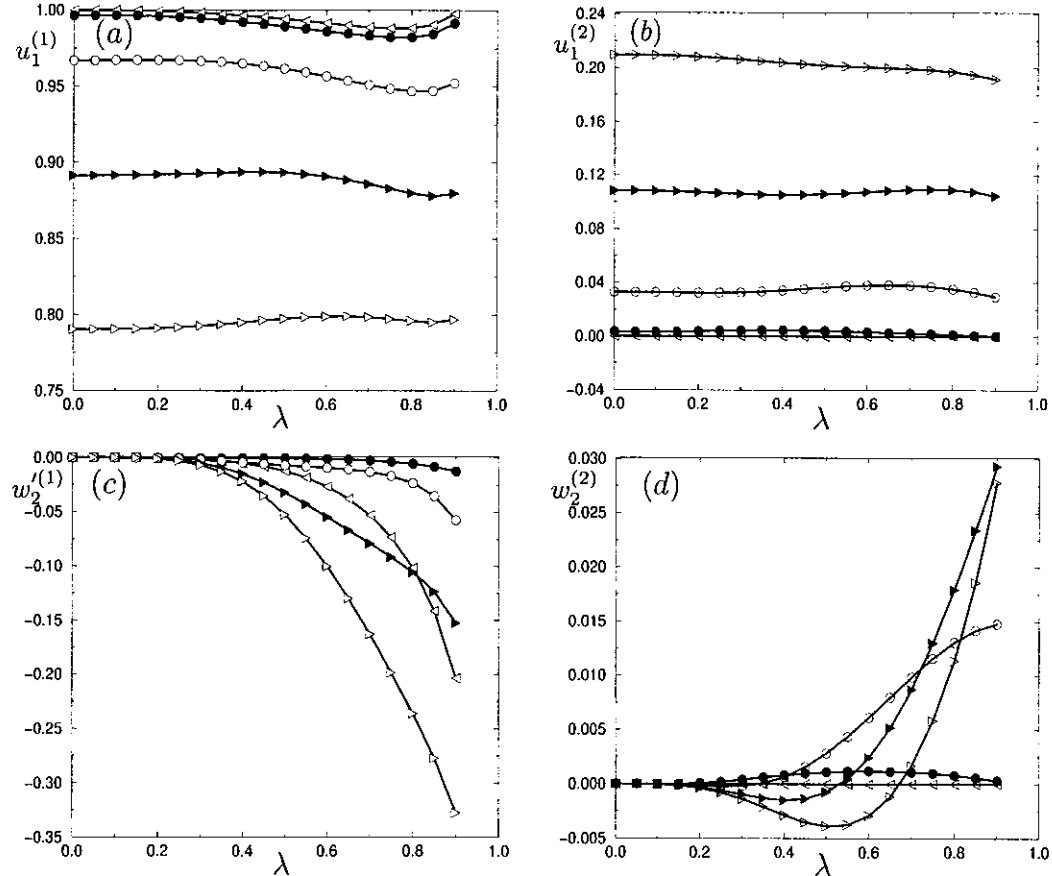


Fig. 2. Non-zero electrophoretic mobilities $u_1^{(n)}$, $w_2^{(2)}$ and $w_2'^{(1)}$ for $d = 0$ (\diamond), $d = 0.3$ (\bullet), $d = 0.6$ (\circ), $d = 0.8$ (\blacktriangleright) or $d = 0.9$ (\triangleright). (a): $u_1^{(1)}$. (b): $u_1^{(2)}$. (c): $w_2'^{(1)}$. (d): $w_2^{(2)}$.

Fig. 2. Mobilités non nulles $u_1^{(n)}$, $w_2^{(2)}$ et $w_2'^{(1)}$ pour $d = 0$ (\diamond), $d = 0.3$ (\bullet), $d = 0.6$ (\circ), $d = 0.8$ (\blacktriangleright) ou $d = 0.9$ (\triangleright). (a) : $u_1^{(1)}$. (b) : $u_1^{(2)}$. (c) : $w_2'^{(1)}$. (d) : $w_2^{(2)}$.

Non-zero mobilities $u_1^{(n)}(d, \lambda)$ and $w_2^{(n)}(d, \lambda)$, computed with $N_1 = N_2 = 866$, are plotted versus λ and for $d = 0, 0.3, 0.6, 0.8$ and 0.9 in Figs. 2(a)–(d). For clarity, our Fig. 2(c) actually displays functions $w_2'^{(1)}(0, \lambda) = w_2^{(1)}(0, \lambda)$ and $w_2'^{(1)}(d, \lambda) = 10[w_2^{(1)}(0, \lambda) - w_2^{(1)}(d, \lambda)]$ for $d > 0$. In view of (1), a single sphere \mathcal{P}_n has mobilities $u_i^{(n)}(0, 0) = \delta_{n1}\delta_{i1}$, $w_i^{(n)}(0, 0) = 0$ (since $\zeta'_n = \delta_{n1}$). Thus, functions $u_1^{(n)} - \delta_{n1}$ and $w_1^{(n)}$ are due to pure sphere–wall (SW) interactions if $d = 0$ and combined sphere–wall and sphere–sphere (SW-SS) interactions if $d > 0$. Note that SW-SS interactions are greater (for $u_1^{(n)}$ and $w_1^{(2)}$; see Figs. 2(a), (b), (d)) or weaker (for $w_1^{(1)}$; see Fig. 2(c)) than SW interactions. For $u_1^{(n)}$ sphere–wall interactions are weak for $0 \leq \lambda \leq 0.9$ (each curve is nearly flat) whereas combined SW-SS interactions, negative for $u_1^{(1)}$ and positive for $u_1^{(2)}$, increase with d up to 20% of the unit Smoluchowski mobility. Mobilities $w_2^{(n)}$ exhibit opposite trends: combined SW-SS interactions (reducing to quantities $w_2^{(n)}$) are weak (less than 3%), positive for \mathcal{P}_1 (remind definition of $w_2'^{(1)}$ and see Fig. 2(c)) and either positive or negative for \mathcal{P}_2 (see Fig. 2(d)).

4. Concluding remarks

Even for our simple “horizontal” 2-sphere cluster, the relative magnitude of particle–particle and particle–wall interactions deeply depends upon the velocity nature (translational or angular). A strong accuracy is needed in all computations and the boundary-integral treatment is quite suitable for such a refined analysis. Finally, particle–particle and wall–particle interactions depend upon the cluster nature (shape and zeta potential of each particle) and orientation relative to \mathbf{E}_∞ and Σ . Such issues are currently investigated.

References

- [1] J.L. Anderson, Colloid transport by interfacial forces, *Ann. Rev. Fluid Mech.* 21 (1989) 61–99.
- [2] M.V. Smoluchowski, in: L. Graetz (Ed.), *Handbuch der Elektrizität und des Magnetismus*, J.A. Barth, Leipzig, 1921.
- [3] F.A. Morrison, Electrophoresis of a particle of arbitrary shape, *J. Colloid Interface Sci.* 34 (1970) 210–214.
- [4] M. Teubner, The motion of charged colloidal particles in electric fields, *J. Chem. Phys.* 76 (11) (1982) 5564–5573.
- [5] J.L. Anderson, Effect of nonuniform zeta potential on particle movements in electric fields, *J. Colloid Interface Sci.* 105 (1985) 45–54.
- [6] L.D. Reed, F.A. Morrison, Hydrodynamic interactions in electrophoresis, *J. Colloid Interface Sci.* 54 (1976) 117–133.
- [7] B. Chen, H.J. Keh, Particles interactions in electrophoresis: I. Motion of two spheres along their line of centers, *J. Colloid Interface Sci.* 130 (2) (1989) 542–555.
- [8] B. Chen, H.J. Keh, Particles interactions in electrophoresis: II. Motion of two spheres normal to their line of centers, *J. Colloid Interface Sci.* 130 (2) (1989) 556–567.
- [9] F.A. Morrison, J.J. Stuckel, Electrophoresis of an insulating sphere normal to a conducting plane, *J. Colloid Interface Sci.* 34 (1970) 210–214.
- [10] H.J. Keh, J.L. Anderson, Boundary effects on electrophoretic motion of colloidal spheres, *J. Fluid Mech.* 153 (1985) 417–439.
- [11] H.J. Keh, S.B. Chen, Electrophoresis of a colloidal sphere parallel to a dielectric plane, *J. Fluid Mech.* 153 (1988) 377–390.
- [12] A. Sellier, On boundary effects in electrophoresis, *C. R. Acad. Sci. Paris, Ser. IIb* 329 (2001) 565–570.
- [13] J. Happel, H. Brenner, *Low Reynolds Number Hydrodynamics*, Martinus Nijhoff, 1973.
- [14] C. Pozrikidis, *Boundary Integral and Singularity Methods for Linearized Viscous Flow*, Cambridge University Press, 1992.
- [15] J.R. Blake, A note on the image system for a Stokeslet in a no-slip boundary, *Proc. Cambridge Phil. Soc.* 70 (1971) 303–310.
- [16] M. Bonnet, *Boundary Integral Equations Methods for Solids and Fluids*, Wiley, 1999.